HHS Public Access

Author manuscript

Brain Pathol. Author manuscript; available in PMC 2021 March 01.

Published in final edited form as:

Brain Pathol. 2020 March ; 30(2): 213–225. doi:10.1111/bpa.12809.

Clinicopathologic and Molecular Features of Intracranial Desmoplastic Small Round Cell Tumors

Julieann C. Lee[1], **Javier E. Villanueva-Meyer**[2], **Sean P. Ferris**[1], **Elaine M. Cham**[3], **Jacob Zucker**[4], **Tabitha Cooney**[5], **Ahmed Gilani**[6], **Bette K. Kleinschmidt-DeMasters**[6], **Dimitri Trembath**[7], **Manuela Mafra**[8], **Jason Chiang**[9], **David W. Ellison**[9], **Soo-Jin Cho**[1], **Andrew E. Horvai**[1], **Jessica Van Ziffle**[1,10], **Courtney Onodera**[1,10], **Patrick Devine**[1,10], **James P. Grenert**[1,10], **Carmen M.A. de Voijs**[11], **W.T. Marja van Blokland**[11], **Wendy W. J. de Leng**[11], **Marieke J. Ploegmakers**[12], **Uta Flucke**[13], **Melike Pekmezci**[1], **Andrew W. Bollen**[1], **Tarik Tihan**[1], **Christian Koelsche**[14], **Andreas von Deimling**[15,16], **Pieter Wesseling**[17], **David A. Solomon**[1,10], **Arie Perry**[1]

[1]Department of Pathology, University of California, San Francisco, CA [2]Department of Radiology and Biomedical Imaging, University of California, San Francisco, CA [3]Department of Pathology, UCSF Benioff Children's Hospital Oakland, Oakland, CA [4]Department of Hematology/Oncology, Renown Children's Hospital, Reno, NV [5]Department of Hematology/Oncology, UCSF Benioff Children's Hospital Oakland, Oakland, CA [6]Department of Pathology, University of Colorado, Denver, CO [7]Department of Pathology, The University of North Carolina at Chapel Hill, Chapel Hill, NC [8]Department of Pathology, The Portuguese Institute of Oncology, Lisbon, Portugal [9]Department of Pathology, St. Jude Children's Research Hospital, Memphis, TN [10]Clinical Cancer Genomics Laboratory, University of California, San Francisco, CA [11]Department of Pathology, University Medical Center Utrecht, Utrecht, The Netherlands [12]Department of Radiology, Radboud University Medical Center Nijmegen, Nijmegen, The Netherlands [13]Department of Pathology, Radboud University Medical Center Nijmegen, Nijmegen, The Netherlands [14]Department of General Pathology, Institute of Pathology, Heidelberg University Hospital, Heidelberg, Germany [15]Clinical Cooperation Unit Neuropathology, German Cancer Research Center (DKFZ), German Consortium for Translational Cancer Research (DKTK), Heidelberg, Germany [16]Department of Neuropathology, Institute of Pathology, Heidelberg University Hospital, Heidelberg, Germany [17]Princess Máxima Center for Pediatric Oncology, Utrecht, and Amsterdam University Medical Centers/VUmc, Amsterdam, The Netherlands

Abstract

To whom correspondence should be addressed: Dr. Arie Perry, MD, Division of Neuropathology, University of California, San Francisco, 505 Parnassus Ave, Room M-551, Box 0102, San Francisco, CA 94143, Phone: 415-476-5236, Fax: 415-476-7963, arie.perry@ucsf.edu.

Data Availability

The data that support the findings of this study are available from the corresponding author upon reasonable request.

Compliance with ethical standards The authors declare no conflict of interest. All procedures performed in studies involving human participants were in accordance with the 1964 Helsinki declaration and its later amendments or comparable ethical standards.

Presented in abstract format at the United States and Canadian Academy of Pathology meeting in National Harbor, Maryland, March 16–21, 2019.

Desmoplastic small round cell tumors (DSRCTs) are highly aggressive sarcomas that most commonly occur intra-abdominally, and are defined by *EWSR1-WT1* gene fusion. Intracranial DSRCTs are exceptionally rare with only seven previously reported fusion-positive cases. Herein, we evaluate the clinical, morphologic, immunohistochemical, and molecular features of five additional examples. All patients were male (age range 6–25 years; median 11 years), with four tumors located supratentorially and one within the posterior fossa. The histologic features were highly variable including small cell, embryonal, clear cell, rhabdoid, anaplastic, and glioma-like appearances. A prominent desmoplastic stroma was seen in only two cases. The mitotic index ranged from <1 to 12/10 HPF (median 5). While all tumors showed strong desmin positivity, epithelial markers such as EMA, CAM 5.2, and other keratins were strongly positive in only one, focally positive in two, and negative in two cases. *EWSR1-WT1* gene fusion was present in all cases, with accompanying mutations in the *TERT* promoter or *STAG2* gene in individual cases. Given the significant histologic diversity, in the absence of genetic evaluation these cases could easily be misinterpreted as other entities. Desmin immunostaining is a useful initial screening method for consideration of a DSRCT diagnosis, prompting confirmatory molecular testing. Demonstrating the presence of an *EWSR1-WT1* fusion provides a definitive diagnosis of DSRCT. Genome-wide methylation profiles of intracranial DSRCTs matched those of extracranial DSRCTs. Thus, despite the occasionally unusual histologic features and immunoprofile, intracranial DSRCTs likely represent a similar, if not the same, entity as their soft tissue counterpart based on the shared fusion and methylation profiles.

Keywords

desmoplastic small round cell tumor; intracranial; *EWSR1-WT1* fusion; desmoplastic stroma; desmin positivity; polyphenotypic

Introduction

Desmoplastic small round cell tumors (DSRCTs) are malignant mesenchymal neoplasms of uncertain histogenesis that most often occur intra-abdominally, with a male to female ratio of approximately 4:1. They are defined by *EWSR1-WT1* gene fusion and display a polyphenotypic immunoprofile with co-expression of epithelial (EMA, cytokeratins), mesenchymal (desmin), and neuronal markers (NSE, synaptophysin) (6, 20, 21, 22, 23, 25, 35, 36, 42, 56). Prior synonyms have emphasized the tumor's unique multilineage immunoprofile and predilection to occur within the abdomen, including desmoplastic small cell tumor with divergent differentiation, polyphenotypic small round cell tumor, and intra-abdominal desmoplastic round cell tumor (6, 25).

The characteristic histologic features of DSRCTs include clusters of small uniform oval cells with hyperchromatic nuclei and scant cytoplasm embedded within a prominent desmoplastic stroma. However, non-classic patterns exist in approximately one third of cases (41). Alternative appearances include epithelioid, spindled, or signet ring-like cells, cellular pleomorphism with marked nuclear atypia, tight paraganglioma-like "Zellballen" nests, Homer Wright-like rosettes, gland formation, papillary growth, or solid sheet-like growth (2, 3, 6, 41, 14). Prominent desmoplasia may be absent in rare examples (3, 41).

DSRCTs are less frequently reported in other locations such as the pleura (31), lung (49), parotid gland (26), kidney (12), pancreas (43), paratesticular region (2, 44), or bone and soft tissues of the extremities (1, 2, 55). Seven intracranial DSRCT cases with confirmation of *EWSR1-WT1* fusion have been reported previously (2, 9, 40, 50, 52). Two other cases reported based on characteristic histology and immunostaining alone (54), or in combination with *EWSR1* rearrangement by FISH (2) may also represent the same entity. Clinical prognosis for patients with abdominal DSRCT has been poor, with a median overall survival of approximately 26 months and 5-year overall survival of 18% (18, 29, 48). Multimodality therapy options utilizing modern surgical and chemotherapy delivery techniques continue to be explored (18, 27).

Materials and Methods

Five cases of intracranial DSRCT, each from a different institution, were evaluated for clinical, morphologic, immunohistochemical, and molecular features. Study inclusion criteria required demonstration of *EWSR1-WT1* fusion either by next-generation sequencing of genomic DNA, or RT-PCR detection of the mRNA fusion transcript. Cases 1–4 had sufficient tumor tissue for genetic evaluation on the UCSF500 Cancer Panel, which assesses approximately 500 cancer-associated genes for mutations, copy number alterations, and structural variants including gene fusions (17, 32, 37, and Supplementary Table 1). Paired tumor-normal sequencing was performed for patient #1 using a buccal swab sample, whereas analysis of tumor tissue only was conducted for patients #2–4. Genomic DNA was extracted from formalin-fixed, paraffin-embedded tumor tissue using the QIAamp DNA FFPE Tissue Kit (Qiagen #56404). Methylation profiling of all five intracranial DSRCT cases was assessed at the University Medical Center Utrecht in The Netherlands using the Illumina EPIC (850k) array and was analyzed by the DKFZ sarcoma classifier for generation of calibrated scores. A detailed list of the entities included in the sarcoma classifier reference cohort is available online (molecularneuropathology.org). For visualization of intracranial DSRCT DNA-methylation data as compared to abdominal/soft tissue DSRCTs and other relevant tumor entities, t-distributed stochastic neighbor embedding (t-SNE) analysis was performed. For case #5, there was only sufficient material for genetic evaluation by RT-PCR and methylation profiling. Copy number changes were evaluated based on results from the UCSF500 Cancer Panel.

Results

The clinical features of the five cases of intracranial DSRCTs are summarized in Table 1. All patients were male (age range 6–25 years; median 11 years). Presenting symptoms were variable and included seizures, headaches, numbness, and weakness. Four tumors were located supratentorially, while one was located within the posterior fossa. Magnetic resonance imaging features ranged from variably enhancing heterogeneous masses with a small cystic component, to multilocular predominantly cystic masses with enhancing solid nodules (Table 1 and Figure 1). All tumors were predominantly parenchymal, with extension to the leptomeninges without overlying dural changes noted in four cases (case #1, #3, #4, and #5). Susceptibility consistent with microhemorrhages was present in case #1, #3, and #4. Case #3 demonstrated reduced diffusion peripherally. For patients #1 and #4 whole body

PET-CT or PET-MRI results were available, which showed no evidence of extracranial malignancy. Patients #4 and #5 underwent gross total resection followed by chemotherapy and radiation, with no evidence of residual disease at 13 months and 8 years after diagnosis respectively. Patient #4 received 6 cycles of vincristine and cyclophosphamide with 55.8 Gy of radiation therapy delivered in 31 fractions (Table 1). Patient #5 received chemotherapy according to the Memorial Sloan-Kettering Cancer Center P6 protocol (34), and 55.8 Gy of radiation therapy with a daily fraction of 1.8 Gy. One patient showed no evidence of disease 16 months after gross total resection and 6 weeks of radiation therapy only. One patient died within one month of surgery, of unspecified causes.

In all five cases the diagnosis of intracranial DSRCT was made after genetic evaluation demonstrated an *EWSR1-WT1* fusion. Initial diagnostic impressions included anaplastic medulloblastoma, astroblastoma-like neoplasm, low-grade tumor with glioneuronal features, malignant tumor NOS, and small round blue cell tumor (Table 2 and Figure 2). Despite the entity's name, a prominent desmoplastic stroma was present in only two cases (case #1 and #4), with the remaining three cases representing the less common "non-desmoplastic variant" or solid-pattern (3, 41). The growth pattern within the brain was either solid, or mixed solid and infiltrative with entrapped axons at the periphery. Cytologic features included cells with hyperchromatic angulated nuclei and indistinctive cell boundaries, clear cells with small bland oval nuclei, small epithelioid cells with amphophilic cytoplasm and oval nuclei, loose areas of low cellularity with spindled tapering bipolar cells, cells with large hyperchromatic pleomorphic nuclei, and cells with small hyperchromatic oval to irregular nuclei within a fibrillar background.

In case #1 (Table 2 and Figure 2) the majority of the tumor appeared glial; there were hyalinized vessels and structures resembling astroblastic pseudorosettes with broad perivascular processes. GFAP staining for this case showed patchy positivity. Other regions contained small round cells embedded in a desmoplastic stroma, indicating a more classical DSRCT appearance at least focally.

Case #3 was located in the posterior fossa, and was diagnostically challenging as the histologic and immunohistochemical features had a remarkable resemblance to an anaplastic medulloblastoma. The tumor cells had large pleomorphic nuclei with abundant mitoses, and features often seen in anaplastic medulloblastomas such as cell-wrapping, apoptotic lakes, and nuclear molding were present (Table 2 and Figure 2). Immunohistochemical studies for medulloblastoma subtyping were performed, which showed strong and diffuse YAP1 staining, moderate GAB1 positivity, cytoplasmic beta-catenin staining, and p53 positivity in 60% of tumor nuclei. A diagnosis of "anaplastic medulloblastoma, SHH-activated and likely TP53-mutant, WHO grade IV" was favored before the case underwent genetic characterization. Rhabdoid features were present focally, a finding that is not uncommon in DSRCTs (21, 41).

Case #2 contained solid sheets of tumor cells with hyperchromatic nuclei, only focal desmoplasia, a high mitotic index, and a malignant appearance. YAP1 immunohistochemistry was also performed in this case, and showed strong diffuse positivity. In contrast, case #4 appeared low-grade (i.e., cytologically bland with low proliferative

activity) with prominent areas of desmoplasia. Case #5 displayed the typical “small round blue cell” appearance; however, this case contained only focal areas of desmoplasia.

The mitotic index ranged from <1 to 12/10 HPF (median 5), and the Ki-67 labeling index ranged from 2% to 80%. The myogenic differentiation marker desmin was strongly positive in all 5 cases, with the globular staining pattern often described for DSRCTs (25, 42) present in case #3. While most cases had strong and diffuse desmin staining, case #1 had strong patchy desmin staining. Staining for the epithelial markers EMA and CAM 5.2 showed strong positivity in only one case (case #3), focal positivity in two cases, and was negative in two cases (Table 2). Staining for neuronal markers showed patchy or focal synaptophysin in 4/5 cases, patchy NeuN in 3/3 cases, and strong CD56 staining in 3/3 cases. GFAP immunostaining performed in four cases (case #1, 3, 4, and 5) showed patchy or focal positivity.

EWSR1-WT1 fusion was detected by targeted next-generation DNA sequencing (4/5) or RT-PCR (1/5) (Table 3). For all cases evaluated by the UCSF500 Cancer panel (case #1, 2, 3, 4), the fusion junction occurred between intron 8–9 of the *EWSR1* gene (NM_013986) on chromosome 22q12 and intron 7–8 of the *WT1* gene (NM_024426) on chromosome 11p33. This fusion is predicted to result in an in-frame fusion protein where the N-terminal portion is composed of exons 1–8 (codons 1–270) of *EWSR1* and the C-terminal portion is composed of exons 8–10 (codons 418–517) of *WT1*. This fusion is identical to the most common *EWSR1-WT1* fusion found in extracranial DSRCTs (4, 22, 24, 35, 39), and only antibodies against the C-terminus of WT1 would be expected to detect WT1 protein expression (39, 56). RT-PCR evaluation of case #5 detected an *EWSR1-WT1* mRNA fusion transcript.

Accompanying pathogenic mutations included a *TERT* promoter hotspot mutation in case #3, and a subclonal *STAG2* splice site mutation in case #4 predicted to disrupt gene function (Table 3). Though case #3 and case #4 both showed staining for p53 in greater than 60% of tumor nuclei, this did not correlate with the presence of an identifiable *TP53* mutation in either case. Case #3 showed multiple chromosomal copy number alterations, while the remaining cases evaluated by the UCSF500 Cancer Panel demonstrated two or fewer chromosomal copy number changes.

Using the DKFZ sarcoma classifier and reference cohort, the methylation profiles of intracranial DSRCTs matched the profiles of extracranial DSRCTs with a calibrated score of 0.99 for all cases. The intracranial and extracranial DSRCT methylation profiles also clustered together by t-distributed stochastic neighbor embedding (t-SNE) analysis (Figure 3).

Discussion

Though DSRCT morphology is characteristically that of a “small round blue cell tumor” with a desmoplastic stroma, non-classic morphologies are known to exist in a subset of cases (2, 3, 6, 14, 41). Therefore, it is important to consider DSRCT in the differential diagnosis not only for “small round blue cell tumors” of the CNS (15, 40), but also for CNS cases with

other morphologies, especially those with a polyphenotypic immunoprofile. We encountered one case in particular that remarkably resembled an anaplastic medulloblastoma, which lacked the desmoplastic stroma usually seen in DSRCT cases (Figure 2, Case #3). This case also illustrated how immunostaining results typically utilized for medulloblastoma subtyping can be misleading if a definitive medulloblastoma diagnosis is not established. This case was positive for YAP1 and GAB1, with p53 positivity in 60% of tumor nuclei, mimicking an anaplastic medulloblastoma, SHH-activated and likely TP53 mutant.

NSE is the neuronal marker typically used during diagnostic evaluation of extracranial DSRCTs, with synaptophysin being less sensitive. Markers such as NSE and CD56 are less often utilized within the CNS due to their lack of specificity. Nevertheless, patchy NeuN and synaptophysin positivity was often found in our intracranial DSRCTs. Polyphenotypic expression is an inherent quality of DSRCTs encountered within the abdomen and soft tissues, with expression of EMA in 94% of 79 cases (23, 42), and expression of CAM 5.2 or AE1/AE2 in 88% of 149 cases (23, 36, 42). Cytokeratin staining in extracranial DSRCT cases usually shows diffuse cytoplasmic staining, occasional dot-like staining, and is rarely only focally positive (36, 42). Of the five intracranial DSRCTs within our series, only one was strongly positive for an epithelial lineage marker. If we also consider the previously published intracranial DSCRTs with confirmed fusion, only six of 12 (50%) have shown strong epithelial antigen positivity. While not all abdominal DSRCTs express epithelial antigens (53), the absence of epithelial antigen positivity is an infrequent finding.

Due to some of the atypical morphologic patterns encountered within this series of intracranial DSRCTs, the suggestion of decreased immunopositivity for epithelial lineage marker expression as compared to intra-abdominal cases, and the unique location of our intracranial *EWSR1-WT1* fusion tumors, we considered the possibility that these cases may represent a distinct entity. Despite sharing the same *EWSR1-WT1* fusion as abdominal DSRCT cases, we postulated that the fundamental biology of intracranial cases could be unique, and thus account for the observed phenotypic differences.

As the methylation profiles of extracranial DSRCTs have been established (33), we compared the methylation profiles of intracranial DSRCT cases to those of extracranial cases, to serve as an additional assessment of similarities in tumor biology. The methylation profiles of intracranial and extracranial DSRCTs were almost identical, with calibrated scores of 0.99. In contrast to our initial hypothesis that these could be distinctive entities with identical genetics and differences in other aspects of their pathology, the shared epigenetic methylation profiles supports that these two groups represent a similar, if not the same, entity at both sites.

As is the case for many neoplasms, the cell of origin for intracranial DSRCTs is not well established. However, one could speculate that a mesenchymal progenitor cell associated with the meninges, the vasculature, or possibly located within the brain parenchyma due to abnormal developmental differentiation or migration, could acquire genetic and epigenetic alterations resulting in sarcoma tumorigenesis. For intra-abdominal DSRCTs a mesothelial or submesothelial origin has been considered (21, 25); which is supported to some degree by expression of desmin and WT1 in both DSRCT and mesothelial cells, and by the

predilection for DSRCT formation within mesothelial-lined cavities. However, DSRCTs also occur in extra-abdominal locations which are not associated with a mesothelial lining, do not show ultrastructural evidence of mesothelial differentiation, and are generally regarded to be of uncertain histogenesis (2, 25, 42, 56).

It may be that the actual number of intracranial DSRCT cases is greater than currently recognized. Due to the variety of morphologic features and radiologic appearances, with both supratentorial and infratentorial locations possible, many cases could go unrecognized. In the absence of genetic evaluation, these cases could easily be misinterpreted as other entities. Since most DSRCTs are strongly desmin positive, desmin immunostaining could be used as an initial screening method to consider the diagnosis.

Desmin positivity, in the context of a polyphenotypic immunoprofile and particularly if there is a globular staining pattern (25, 42), is highly suggestive of a DSRCT diagnosis. However, a polyphenotypic immuneprofile with desmin positivity is not specific to DSRCT, and can also be encountered in angiomatous fibrous histiocytoma, intracranial myxoid mesenchymal tumors, and sarcomas with *EWSR1-PATZ1* gene fusion (7, 11, 19, 30). We encountered two such cases while establishing our DSRCT study cohort, which were desmin positive but demonstrated an *EWSR1-ATF1* gene fusion on molecular evaluation, one of these cases also had a prominent desmoplastic stroma. Desmin positivity could be very useful as an initial screening test, which would then initiate additional confirmatory molecular testing to evaluate for the presence of an *EWSR1-WT1* gene fusion, a matching methylation profile, or surrogate indication of the fusion by WT1 immunostaining.

Utilizing a WT1 antibody that specifically recognizes the C-terminus of WT1 detects nuclear positivity in many cases of DSRCT with confirmed *EWSR1-WT1* gene fusion (39, 56), with sensitivity ranging from 70–100% depending on the study (56, 8, 28). Specificity for DSRCT was also high when compared to peripherally located neoplasms including rhabdomyosarcoma, Ewing sarcoma, neuroblastoma, and rhabdoid tumors of the kidney, with the exception being that nephroblastomas also show nuclear WT1 positivity (8, 28). However, caution must be utilized in relying on immunohistochemistry alone, as it is important to recognize that WT1 antibodies directed against the N-terminus of WT1 will not recognized the nuclear fusion protein generated by transcription/translation of an *EWSR1-WT1* gene fusion containing the C-terminal exons of WT1 (39, 56). A WT1 antibody appropriately targeted against the C-terminus is a less expensive and rapid analysis option for immunohistochemical indication of *EWSR1-WT1* fusion in medical centers without molecular testing techniques.

Demonstrating the presence of an *EWSR1-WT1* fusion provides a definitive diagnosis of DSRCT. An important caveat is that establishing the presence of an *EWSR1* gene rearrangement by break-apart FISH probes alone is insufficient, as other *EWSR1* fusion tumors can closely resemble a DSRCT by both histologic features and immunostaining. This is especially relevant for angiomatous fibrous histiocytoma, and for intracranial myxoid mesenchymal tumors with *EWSR1-CREB* family gene fusions (7, 19, 30). As previously mentioned, these tumors can have a desmoplastic stroma and show polyphenotypic differentiation with desmin positivity, and would also be positive for *EWSR1* gene

rearrangement by break-apart FISH. Intra-abdominal sarcomas with *EWSR1-PATZ1* gene fusion have also shown similar histologic features and immunostaining results, and similarly would show an *EWSR1* rearrangement by break-apart FISH (11).

In addition to the *EWSR1-WT1* gene fusion within our 5 cases, accompanying pathogenic mutations of the *TERT* promoter or *STAG2* gene were demonstrated in individual cases. *STAG2* encodes a core subunit of the cohesin complex that regulates chromatid cohesion, segregation, and architecture (38, 47). Inactivating mutations in *STAG2* are the most frequent accompanying somatic mutation in Ewing sarcoma, occurring in approximately 17% of cases, and are associated with poor outcome (10, 51). To the best of our knowledge, among the relatively few cases of DSRCT that have either undergone extensive genetic sequencing (13, 16, 46) or sequencing focused specifically on accompanying *STAG2 or TP53* mutations (45), only one additional case with a *STAG2* mutation has been reported (45). This patient's *EWSR1-WT1* gene fusion and accompanying inactivating *STAG2* splice site mutation were detected within tumor tissue and within plasma derived cell free DNA (45). The prognostic implication of accompanying *STAG2* mutations within DSRCT is of uncertain significance. Within our review of DSRCT sequencing studies available in the literature, whole exome sequencing analysis was performed on seven tumors (13, 16), a targeted panel of cancer related genes were assessed in one tumor (46), and 6 tumors were evaluated specifically for accompanying *STAG2* or *TP53* mutations using a targeted cancer panel (45). Mutation of the *TERT* promoter was either not identified or not assessed in these studies, and would not be detected by sequencing limited to the exome.

Though prognosis for patients with abdominal DSRCTs has been well-studied (18, 48, 27, 29), prediction of clinical outcomes for intracranial DSRCTs is currently limited by the small number of reported cases. Of the 12 genetically confirmed cases within the literature including this series (2, 9, 40, 50, 52), four patients died at 1 month, 20 months, 2 years, and 2.6 years after diagnosis (2, 40, 50). One patient was alive with progressive disease at 27 months (40). Four patients were alive with no evidence of disease at 13 months, 16 months, 18 months (9, 50), and 8 years. One patient was alive with no clinical signs of relapse at approximately 3 years (50, 52). For two patients clinical follow-up was not available. Among these 12 patients, one developed spinal dissemination, one patient who had leptomeningeal deposits at presentation developed progressive disease (40), one patient developed recurrent disease with lymph node metastases (50), and one had vertebral metastatic disease (2). A summary of the clinical, histologic, and molecular findings for the seven previously reported cases of *EWSR1-WT1* fusion-positive intracranial DSRCTs is provided within Table 4 (2, 9, 40, 50, 52).

In summary, the histologic features of intracranial DSRCTs can be highly variable, and therefore a high index of suspicion is required for cases that lack the classical appearance. Intracranial DSRCTs with *EWSR1-WT1* fusion may not have the same degree of epithelial lineage marker expression as seen in intra-abdominal cases. Despite differences in the morphologic appearance and immunostaining profile, methylation analysis supports that intracranial DSRCTs represent a similar, if not the same, entity as DSRCTs seen elsewhere in the body.

Supplementary Material

Refer to Web version on PubMed Central for supplementary material.

Acknowledgements

This study was supported in part by the NIH Director's Early Independence Award (DP5 OD021403) to D.A.S. We thank the staff of the UCSF Clinical Cancer Genomics Laboratory for assistance with genetic profiling, and the staff of the Molecular Pathology Laboratory of the University Medical Center Utrecht for their help with methylation profiling.

REFERENCES

1. Adsay V, Cheng J, Athanasian E, Gerald W, Rosai J (1999) Primary desmoplastic small cell tumor of soft tissues and bone of the hand. Am J Surg Pathol. 11;23(11):1408–13. [PubMed: 10555010]
2. Al-Ibraheemi A, Broehm C, Tanas MR, Horvai AE, Rubin BP, Cheah AL, et al. (2019) Desmoplastic Small Round Cell Tumors With Atypical Presentations: A Report of 34 Cases. Int J Surg Pathol. 27(3):236–243. [PubMed: 30522375]
3. Ali A, Mohamed M, Chisholm J, Thway K (2017) Solid-Pattern Desmoplastic Small Round Cell Tumor. Int J Surg Pathol. 4;25(2):158–161. [PubMed: 27431755]
4. Antonescu CR, Gerald WL, Magid MS, Ladanyi M (1998) Molecular variants of the EWS-WT1 gene fusion in desmoplastic small round cell tumor. Diagn Mol Pathol. 2;7(1):24–8. [PubMed: 9646031]
5. Antonescu CR, Dal Cin P, Nafa K, Teot LA, Surti U, Fletcher CD, Ladanyi M (2007) EWSR1-CREB1 is the predominant gene fusion in angiomatoid fibrous histiocytoma.Genes Chromosomes Cancer. 12;46(12):1051–60. [PubMed: 17724745]
6. Antonescu CR, Ladanyi M (2012) Desmoplastic small round cell tumor In: WHO Classification of Tumours of Soft Tissue and Bone, Fletcher DM, Bridge JA, Hogendoorn CW, Mertens F (eds) pp.225–227, International Agency for Research on Cancer: Lyon, France.
7. Bale TA, Oviedo A, Kozakewich H, Giannini C, Davineni PK, Ligon K, Alexandrescu S (2018) Intracranial myxoid mesenchymal tumors with EWSR1-CREB family gene fusions: myxoid variant of angiomatoid fibrous histiocytoma or novel entity? Brain Pathol. 3;28(2):183–191. [PubMed: 28281318]
8. Barnoud R, Sabourin JC, Pasquier D, Ranchère D, Bailly C, Terrier-Lacombe MJ, Pasquier B (2000) Immunohistochemical expression of WT1 by desmoplastic small round cell tumor: a comparative study with other small round cell tumors. Am J Surg Pathol 6;24(6):830–6. [PubMed: 10843285]
9. Bouchireb K, Auger N, Bhangoo R, Di Rocco F, Brousse N, Delattre O, et al. (2008) Intracerebral small round cell tumor: an unusual case with EWS-WT1 translocation. Pediatr Blood Cancer 51(4):545–8. [PubMed: 18561179]
10. Brohl AS, Solomon DA, Chang W, Wang J, Song Y, Sindiri S, et al. (2014) The genomic landscape of the Ewing Sarcoma family of tumors reveals recurrent STAG2 mutation. PLoS Genet. 7 10;10(7):e1004475.
11. Chougule A, Taylor MS, Nardi V, Chebib I, Cote GM, Choy E, et al. (2019) Spindle and Round Cell Sarcoma With EWSR1-PATZ1 Gene Fusion: A Sarcoma With Polyphenotypic Differentiation. Am J Surg Pathol. 43(2):220–228. [PubMed: 30379650]
12. Collardeau-Frachon S, Ranchère-Vince D, Delattre O, Hoarau S, Thiesse P, Dubois R et al. (2007) Primary desmoplastic small round cell tumor of the kidney: a case report in a 14-year-old girl with molecular confirmation. Pediatr Dev Pathol. Jul-Aug;10(4):320–4. [PubMed: 17638432]
13. Devecchi A, De Cecco L, Dugo M, Penso D, Dagrada G, Brich S, et al. (2018) The genomics of desmoplastic small round cell tumor reveals the deregulation of genes related to DNA damage response, epithelial-mesenchymal transition, and immune response. Cancer Commun (Lond). 11 28;38(1):70. [PubMed: 30486883]

14. Dorsey BV, Benjamin LE, Rauscher F III, Klencke B, Venook AP, Warren RS, Weidner N (1996) Intra-abdominal desmoplastic small round-cell tumor: expansion of the pathologic profile. Mod Pathol. 6;9(6):703–9. [PubMed: 8782211]
15. Dunham C (2015) Uncommon pediatric tumors of the posterior fossa: pathologic and molecular features. Childs Nerv Syst 31(10):1729–37. [PubMed: 26351226]
16. Ferreira EN, Barros BD, de Souza JE, Almeida RV, Torrezan GT, Garcia S, et al. (2016) A genomic case study of desmoplastic small round cell tumor: comprehensive analysis reveals insights into potential therapeutic targets and development of a monitoring tool for a rare and aggressive disease. Hum Genomics 11 18;10(1):36. [PubMed: 27863505]
17. Ferris SP, Velazquez Vega J, Aboian M, Lee JC, Van Ziffle J, Onodera C, et al. (2019) High-grade neuroepithelial tumor with BCOR exon 15 internal tandem duplication-a comprehensive clinical, radiographic, pathologic, and genomic analysis. Brain Pathol. 2019 5 18. [Epub ahead of print].
18. Gani F, Goel U, Canner JK, Meyer CF, Johnston FM (2019) A national analysis of patterns of care and outcomes for adults diagnosed with desmoplastic small round cell tumors in the United States. J Surg Oncol. 6;119(7):880–886. [PubMed: 30844086]
19. Gareton A, Pierron G, Mokhtari K, Tran S, Tauziède-Espariat A, Pallud J, et al. (2018) ESWR1-CREM Fusion in an Intracranial Myxoid Angiomatoid Fibrous Histiocytoma-Like Tumor: A Case Report and Literature Review. J Neuropathol Exp Neurol. 2018 7 1;77(7):537–541. [PubMed: 29788195]
20. Gerald WL, Rosai J (1989) Case 2. Desmoplastic small cell tumor with divergent differentiation. Pediatr Pathol. 9(2):177–83. [PubMed: 2473463]
21. Gerald WL, Miller HK, Battifora H, Miettinen M, Silva EG, Rosai J (1991) Intra-abdominal desmoplastic small round-cell tumor. Report of 19 cases of a distinctive type of high-grade polyphenotypic malignancy affecting young individuals. Am J Surg Pathol. 6;15(6):499–513. [PubMed: 1709557]
22. Gerald WL, Rosai J, Ladanyi M (1995) Characterization of the genomic breakpoint and chimeric transcripts in the EWS-WT1 gene fusion of desmoplastic small round cell tumor. Proc Natl Acad Sci U S A 92(4):1028–32. [PubMed: 7862627]
23. Gerald WL, Ladanyi M, de Alava E, Cuatrecasas M, Kushner BH, LaQuaglia MP, Rosai J (1998) Clinical, pathologic, and molecular spectrum of tumors associated with t(11;22)(p13;q12): desmoplastic small round-cell tumor and its variants. J Clin Oncol 16(9):3028–36. [PubMed: 9738572]
24. Gerald WL and Haber DA (2005) The EWS-WT1 gene fusion in desmoplastic small round cell tumor. Semin Cancer Biol 15(3):197–205. [PubMed: 15826834]
25. Goldblum JR, Folpe AL, Weiss SW(eds) (2014) Desmoplastic small round cell tumor In: Enzinger & Weiss's Soft Tissue Tumors. Chapter 33, pp.1079–1084, Elsevier Saunders: Philadelphia, PA.
26. Hatanaka KC, Takakuwa E, Hatanaka Y, Suzuki A, IIzuka S, Tsushima N et al. (2019) Desmoplastic small round cell tumor of the parotid gland-report of a rare case and a review of the literature. Diagn Pathol. 5 18;14(1):43. [PubMed: 31103034]
27. Hayes-Jordan AA, Coakley BA, Green HL, Xiao L, Fournier KF, Herzog CE et al. (2018) Desmoplastic Small Round Cell Tumor Treated with Cytoreductive Surgery and Hyperthermic Intraperitoneal Chemotherapy: Results of a Phase 2 Trial. Ann Surg Oncol. 4;25(4):872–877.
28. Hill DA, Pfeifer JD, Marley EF, Dehner LP, Humphrey PA, Zhu X, Swanson PE (2000) WT1 staining reliably differentiates desmoplastic small round cell tumor from Ewing sarcoma/primitive neuroectodermal tumor. An immunohistochemical and molecular diagnostic study. Am J Clin Pathol 9;114(3):345–53. [PubMed: 10989634]
29. Honoré C, Amroun K, Vilcot L, Mir O, Domont J, Terrier P et al. (2015) Abdominal desmoplastic small round cell tumor: multimodal treatment combining chemotherapy, surgery, and radiotherapy is the best option. Ann Surg Oncol. 2015 4;22(4):1073–9. [PubMed: 25300608]
30. Kao YC, Sung YS, Zhang L, Chen CL, Vaiyapuri S, Rosenblum MK, Antonescu CR (2017) EWSR1 Fusions With CREB Family Transcription Factors Define a Novel Myxoid Mesenchymal Tumor With Predilection for Intracranial Location. Am J Surg Pathol. 4;41(4):482–490. [PubMed: 28009602]

31. Karavitakis EM, Moschovi M, Stefanaki K, Karamolegou K, Dimitriadis E, Pandis N et al. (2007) Desmoplastic small round cell tumor of the pleura. Pediatr Blood Cancer. 9;49(3):335–8. [PubMed: 16429445]
32. Kline CN, Joseph NM, Grenert JP, van Ziffle J, Talevich E, Onodera C et al. (2017) Targeted next-generation sequencing of pediatric neuro-oncology patients improves diagnosis, identifies pathogenic germline mutations, and directs targeted therapy. Neuro-Oncol 19:699–709. [PubMed: 28453743]
33. Koelsche C, Hartmann W, Schrimpf D, Stichel D, Jabar S, Ranft A et al. (2018) Array-based DNA-methylation profiling in sarcomas with small blue round cell histology provides valuable diagnostic information. Mod Pathol. 2018 8;31(8):1246–1256. [PubMed: 29572501]
34. Kushner BH, LaQuaglia MP, Wollner N, Meyers PA, Lindsley KL, Ghavimi F et al. (1996) Desmoplastic small round-cell tumor: prolonged progression-free survival with aggressive multimodality therapy. J Clin Oncol. 14(5):1526–31. [PubMed: 8622067]
35. Ladanyi M and Gerald W (1994) Fusion of the EWS and WT1 genes in the desmoplastic small round cell tumor. Cancer Res 54(11):2837–40. [PubMed: 8187063]
36. Lae ME, Roche PC, Jin L, Lloyd RV, Nascimento AG (2002) Desmoplastic small round cell tumor: a clinicopathologic, immunohistochemical, and molecular study of 32 tumors. Am J Surg Pathol. 7;26(7):823–35. [PubMed: 12131150]
37. Lee JC, Villanueva-Meyer JE, Ferris SP, Sloan EA, Hofmann JW, Hattab EM et al. (2019) Primary intracranial sarcomas with DICER1 mutation often contain prominent eosinophilic cytoplasmic globules and can occur in the setting of neurofibromatosis type 1. Acta Neuropathol 137(3):521–525. [PubMed: 30649606]
38. Mondal G, Stevers M, Goode B, Ashworth A, Solomon DA (2019) A requirement for STAG2 in replication fork progression creates a targetable synthetic lethality in cohesin-mutant cancers. Nat Commun. 2019 4 11;10(1):1686. [PubMed: 30975996]
39. Murphy AJ, Bishop K, Pereira C, Chilton-MacNeill S, Ho M, Zielenska M, Thorner PS. A new molecular variant of desmoplastic small round cell tumor: significance of WT1 immunostaining in this entity. Hum Pathol 39(12):1763–70.
40. Neder L, Scheithauer BW, Turel KE, Arnesen MA, Ketterling RP, Jin L, et al. (2009) Desmoplastic small round cell tumor of the central nervous system: report of two cases and review of the literature. Virchows Arch 454(4):431–9. [PubMed: 19263077]
41. Ordóñez NG (1998) Desmoplastic small round cell tumor: I: a histopathologic study of 39 cases with emphasis on unusual histological patterns. Am J Surg Pathol 22(11):1303–13. [PubMed: 9808123]
42. Ordóñez NG (1998) Desmoplastic small round cell tumor: II: an ultrastructural and immunohistochemical study with emphasis on new immunohistochemical markers. Am J Surg Pathol 22(11):1314–27. [PubMed: 9808124]
43. Ryan A, Razak A, Graham J, Benson A, Rowe D, Haugk B, Verrill M (2007) Desmoplastic small round-cell tumor of the pancreas. J Clin Oncol. 4 10;25(11):1440–2. [PubMed: 17416866]
44. Sedig L, Geiger J, Mody R, Jasty-Rao R (2017) Paratesticular desmoplastic small round cell tumors: A case report and review of the literature. Pediatr Blood Cancer. 12;64(12).
45. Shukla NN, Patel JA, Magnan H, Zehir A, You D, Tang J, et al. (2017) Plasma DNA-based molecular diagnosis, prognostication, and monitoring of patients with EWSR1 fusion-positive sarcomas. JCO Precis Oncol. 2017.
46. Silva JG, Corrales-Medina FF, Maher OM, Tannir N, Huh WW, Rytting ME, Subbiah V. (2015) Clinical next generation sequencing of pediatric-type malignancies in adult patients identifies novel somatic aberrations. Oncoscience 2 20;2(2):187–92. [PubMed: 25859559]
47. Solomon DA, Kim T, Diaz-Martinez LA, Fair J, Elkahloun AG, Harris BT, et al. (2011) Mutational inactivation of STAG2 causes aneuploidy in human cancer. Science 8;333(6045):1039–43. [PubMed: 21852505]
48. Stiles ZE, Dickson PV, Glazer ES, Murphy AJ, Davidoff AM, Behrman SW et al. (2018) Desmoplastic small round cell tumor: A nationwide study of a rare sarcoma. J Surg Oncol. 6;117(8):1759–1767. [PubMed: 29878371]

49. Syed S, Haque AK, Hawkins HK, Sorensen PH, Cowan DF (2002) Desmoplastic small round cell tumor of the lung. Arch Pathol Lab Med. 10;126(10):1226–8. [PubMed: 12296765]
50. Thondam SK, du Plessis D, Cuthbertson DJ, Das KS, Javadpour M, MacFarlane IA, et al. (2015) Intracranial desmoplastic small round cell tumor presenting as a suprasellar mass. J Neurosurg 122(4):773–7. [PubMed: 25479120]
51. Tirode F, Surdez D, Ma X, Parker M, Le Deley MC, Bahrami A, et al. (2014) Genomic landscape of Ewing sarcoma defines an aggressive subtype with co-association of STAG2 and TP53 mutations. Cancer Discov. 11;4(11):1342–53. [PubMed: 25223734]
52. Tison V, Cerasoli S, Morigi F, Ladanyi M, Gerald WL, Rosai J (1996) Intracranial desmoplastic small-cell tumor. Report of a case. Am J Surg Pathol 20(1):112–7. [PubMed: 8540602]
53. Trupiano JK, Machen SK, Barr FG, Goldblum JR (1999) Cytokeratin-negative desmoplastic small round cell tumor: a report of two cases emphasizing the utility of reverse transcriptase-polymerase chain reaction. Mod Pathol. 9;12(9):849–53. [PubMed: 10496592]
54. Yachnis AT, Rorke LB, Biegel JA, Perilongo G, Zimmerman RA, Sutton LN (1992) Desmoplastic primitive neuroectodermal tumor with divergent differentiation. Broadening the spectrum of desmoplastic infantile neuroepithelial tumors. Am J Surg Pathol 16(10):998–1006. [PubMed: 1384373]
55. Yoshida A, Edgar MA, Garcia J, Meyers PA, Morris CD, Panicek DM (2008) Primary desmoplastic small round cell tumor of the femur. Skeletal Radiol. 9;37(9):857–62. [PubMed: 18470511]
56. Zhang PJ, Goldblum JR, Pawel BR, Fisher C, Pasha TL, Barr FG (2003) Immunophenotype of desmoplastic small round cell tumors as detected in cases with EWS-WT1 gene fusion product. Mod Pathol 16(3):229–35. [PubMed: 12640103]

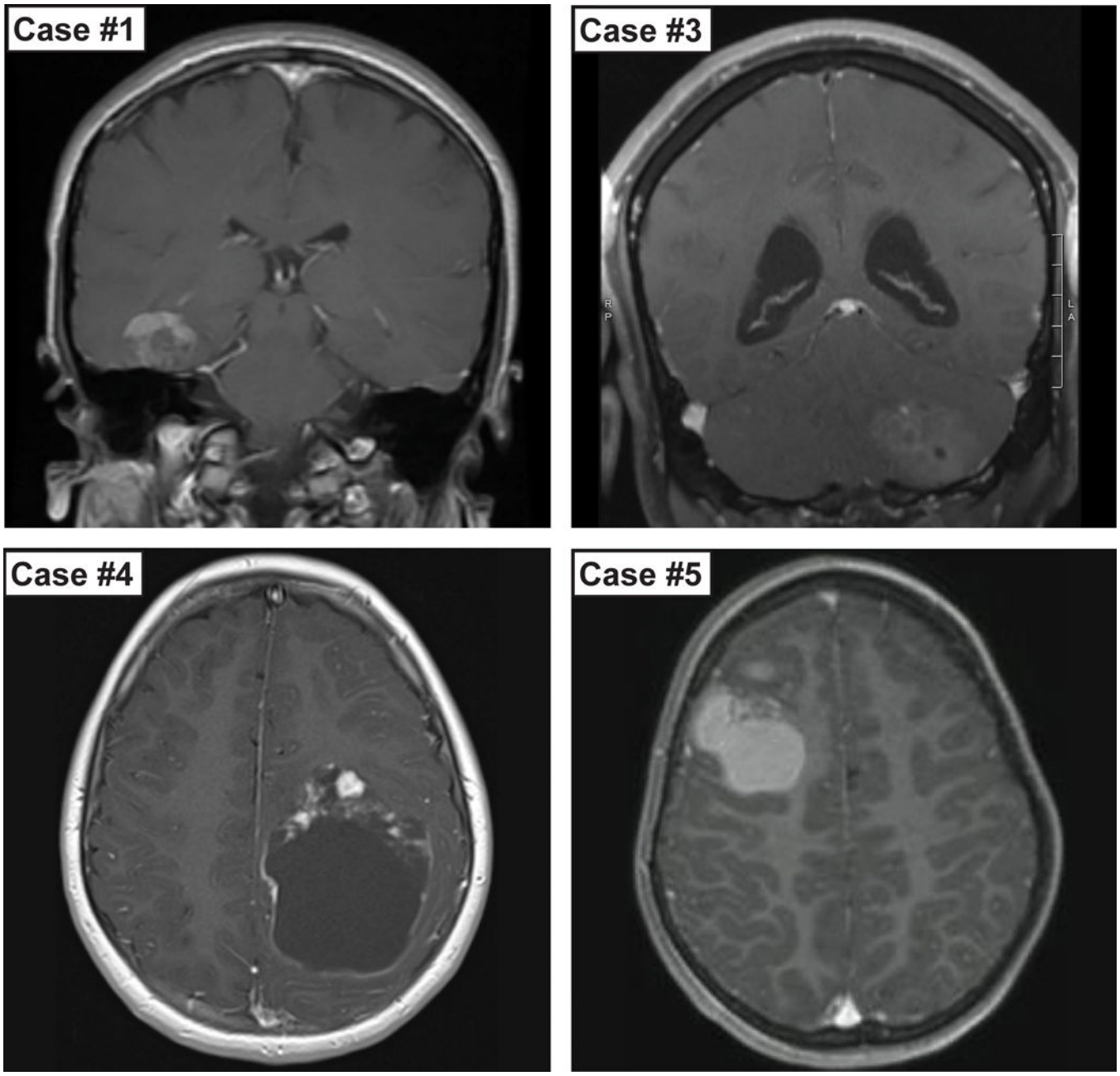

Figure 1.

Representative pre-operative imaging from four cases of intracranial DSRCTs, showing T1 weighted MRIs with contrast. Images demonstrate the variety of radiologic findings including supratentorial and infratentorial locations, the variable degree of a cystic component, and relative degree of enhancement. Case #1: A right temporal heterogeneously enhancing mass. Case #3: A left cerebellar heterogeneous minimally enhancing mass. Case #4: A left parietal cystic mass with enhancing nodules. Case #5: A right frontal intrinsically T1 hyperintense mass with only focal nodular enhancement.

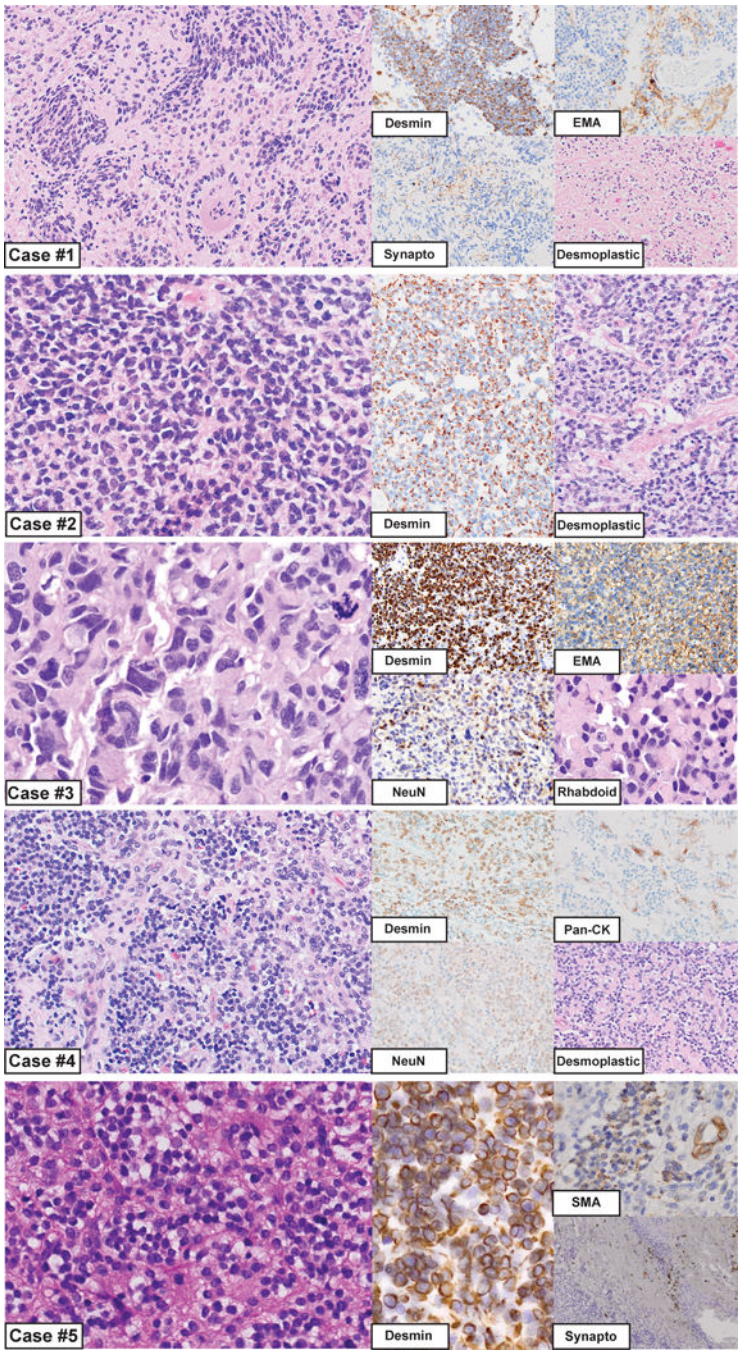

Figure 2.

Morphologic appearance of intracranial DSRCTs for cases 1–5. Case #1: Regions of this tumor resembled an astroblastoma-like glial neoplasm, while in other areas there was a markedly desmoplastic stroma with interspersed small round cells. Immunostaining for desmin, EMA, and synaptophysin are shown. Case #2: This tumor had a uniform solid appearance with sheets of hyperchromatic nuclei, and only focal areas of mild desmoplasia. Desmin was strong and diffusely positive. Case #3: The histology of this case resembled an anaplastic medulloblastoma, including cell-wrapping, large cells, and nuclear molding.

Rhabdoid features were appreciated focally; however, a desmoplastic stroma was not present in this case. Immunostaining for desmin, EMA, and NeuN are shown, depicting the globular desmin staining that is often described for DSRCTs. This was the only case in our series with extensive epithelial marker expression. Case #4: This tumor appeared low grade with prominent areas of desmoplasia. Immunostaining for desmin, pan-cytokeratin, and NeuN are shown. Case #5: These tumor cells contained small round blue nuclei, and there were focal areas of desmoplasia. Immunostaining for desmin, SMA, and synaptophysin are shown.

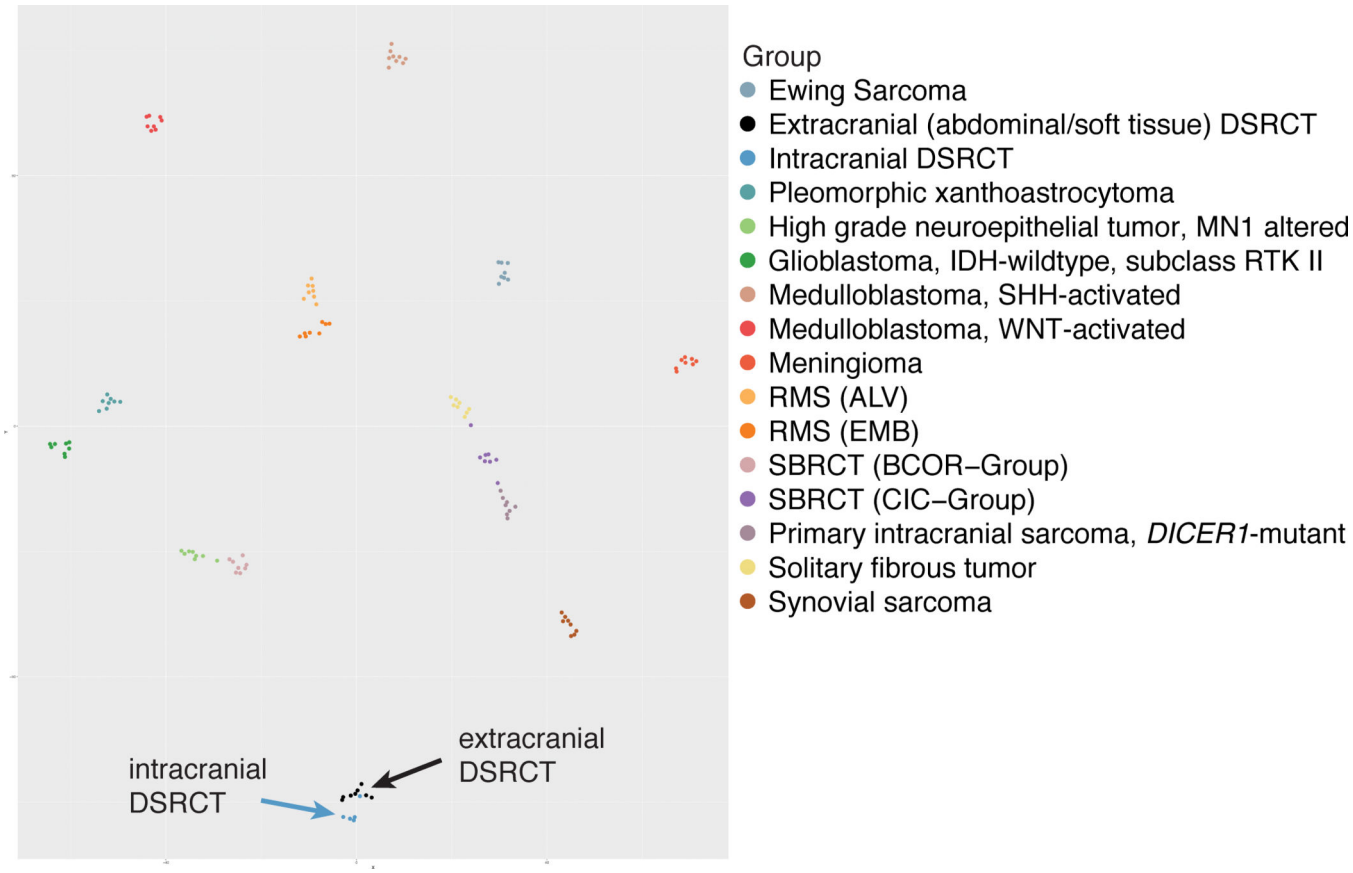

Figure 3.

DNA-methylation profiling data visualized by t-distributed stochastic neighbor embedding (t-SNE), for comparison of DSRCTs located intracranially (dark blue circles) to those occurring extracranially within the abdomen and soft tissues (black circles). Other relevant CNS and soft tissue tumor entities are also shown. Abbreviations: DSRCT: Desmoplastic small round cell tumor, RMS (ALV): alveolar rhabdomyosarcoma, RMS (EMB): embryonal rhabdomyosarcoma, SBRCT (BCOR−Group): Small blue round cell tumor with *BCOR* alteration, SBRCT (CIC−Group): Small blue round cell tumor with *CIC* alteration.

Table 1.

Clinical and radiologic features of the five intracranial DSRCTs within our series. Available clinical and radiologic information, including the status at last follow-up and length of follow-up interval, is depicted. The Memorial Sloan-Kettering Cancer Center (MSKCC) P6 protocol has seven courses of chemotherapy. Courses 1, 2, 3, and 6 included cyclophosphamide 4,200 mg/m^2, doxorubicin 75 mg/m^2, and vincristine. Courses 4, 5, and 7 consisted of ifosfamide 9 g/m^2 and etoposide 500 mg/m^2 for previously untreated patients (34). The symbol "-" is used to indicate when selected information was not available. XRT: radiation therapy. Gy: gray. MSKCC: Memorial Sloan-Kettering Cancer Center.

Case #	Age (years)	Gender	Tumor location	Size (cm)	Presenting symptoms	Imaging findings at presentation	Extent of resection	Adjuvant chemotherapy	Adjuvant radiation therapy	Clinical status	Length of follow-up
1	13	M	right temporal	4.3	seizures	solid and cystic mass, heterogeneous nodular enhancement	gross total	none	6 weeks of radiation therapy (XRT)	no evidence of disease	16 months
2	6	M	left occipital	6.3	-	heterogeneous mass (contrast not administered)	-	-	-	-	-
3	25	M	left cerebellum	4.7	left hand numbness, headaches	heterogeneous mass, minimal nodular enhancement	gross total	none	none	deceased	1 month
4	11	M	left parietal	8.5	progressive right-sided weakness	multilocular cystic mass with enhancing nodules	gross total	6 cycles of vincristine and cyclophosphamide	XRT, 55.8 Gy in 31 fractions	no evidence of disease	13 months
5	8	M	right frontal	-	headaches	T1 hyperintense cystic mass with focal enhancement	gross total	MSKCC P6 protocol	XRT, 55.8 Gy with a daily fraction of 1.8 Gy	no evidence of disease	8 years

Table 2.

Histologic and immunohistochemical features of the five intracranial DSRCTs within our series.

Case #	Initial diagnostic impression	Desmoplastic stroma	Mitotic index	Ki-67 LI	Necrosis	myogenic markers	Epithelial markers	Neuronal markers
1	Glial neoplasm with an astroblastoma-like pattern	Markedly desmoplastic stroma	Less than 1/10 HPFs	2%	Not present	Desmin: patchy strong positivity	EMA: focal CAM 5.2: negative Cytokeratin MCK: negative	Synaptophysin: focal NeuN: patchy Neurofilament: negative CD56: positive
2	Malignant tumor, not otherwise specified (NOS)	Only focal desmoplasia	10/10 HPFs	-	Foci of necrosis	Desmin: diffusely positive	EMA: negative CAM 5.2: negative AE1/AE3: negative	Synaptophysin: negative
3	Favor anaplastic medulloblastoma, WHO grade IV	Not present	12/10 HPFs	80%	Foci of necrosis	Desmin: diffusely positive SMA: negative	EMA: extensively positive CAM 5.2: patchy CK7: focal CK20: focal	Synaptophysin: patchy NeuN: patchy Neurofilament: patchy
4	Low-grade glioneuronal tumor	Markedly desmoplastic stroma	Less than 1/10 HPFs	8%	Not present	Desmin: diffusely positive Myogenin: negative	EMA: focal CAM 5.2: negative Pan-cytokeratin: focal	Synaptophysin: focal NeuN: patchy Neurofilament: negative CD56: positive
5	Small round blue cell tumor	Only focal desmoplasia	-	-	-	Desmin: strongly positive Myogenin: negative SMA: focally positive	EMA: negative CAM 5.2: negative Pan-cytokeratin: negative	Synaptophysin: focal CD56: positive

Table 3.

Molecular features of intracranial DSRCTs, including methylation profiling calibrated scores as analyzed by the DKFZ sarcoma classifier (molecularneuropathology.org), fusions, pathogenic mutations, and copy number alterations. For cases 1–4 the *EWSR1-WT1* gene fusion was detected by the UCSF500 Cancer Panel, for case #5 the *EWSR1-WT1* fusion transcript was detected by RT-PCR. The symbol "-" is used to indicate when selected information was not available.

Case #	Methylation profile DKFZ Sarcoma Classifier	Fusions	Pathogenic mutations	Copy number alterations
1	Desmoplastic small round cell tumor (calibrated score of 0.99)	EWSR1-WT1 gene fusion NM_013986, NM_024426 intron 8–9 of EWSR1 to intron 7–8 of WT1 334 reads over fusion junction	none	Loss of 8p
2	Desmoplastic small round cell tumor (calibrated score of 0.99)	EWSR1-WT1 gene fusion NM_013986, NM_024426 intron 8–9 of EWSR1 to intron 7–8 of WT 1 229 reads over fusion junction	none	none
3	Desmoplastic small round cell tumor (calibrated score of 0.99)	EWSR1-WT1 gene fusion NM_013986, NM_024426 intron 8–9 of EWSR1 to intron 7–8 of WT 1 191 reads over fusion junction	TERT promoter hotspot mutation c.-124C>T NM_198253 796 reads, 28% MAF	Gains of proximal 1p, 1q, 2, 5, 7, proximal 11p, 11q, 15, 18, 19, 20, 21, and distal 22q Losses of distal 1p, 16, and 17
4	Desmoplastic small round cell tumor (calibrated score of 0.99)	EWSR1-WT1 gene fusion NM_013986, NM_024426 intron 8–9 of EWSR1 to intron 7–8 of WT 1 389 reads over fusion junction	STAG2 splice site mutation c.3278- 1G>A NM_001042749 480 reads, 19% MAF	Gain of 1q and loss of 20p
5	Desmoplastic small round cell tumor (calibrated score of 0.99)	EWSR1-WT1 fusion transcript	-	-

Table 4.

brief summary of the available clinical, radiologic, histologic, immunohistochemical, and molecular features for the seven previously reported cases of *WSR1-WT1* fusion-positive intracranial DSRCTs is provided within Table 4 (2, 9, 40, 50, 52), which is adapted from Thondam et al., 2015. Two other ses reported in the literature based on characteristic histology and immunostaining alone (54), or in combination with *EWSR1* rearrangement by FISH may also represent the same entity. The Memorial Sloan-Kettering Cancer Center (MSKCC) P6 protocol has seven courses of chemotherapy. Courses 2, 3, and 6 included cyclophosphamide 4,200 mg/m^2, doxorubicin 75 mg/m^2, and vincristine. Courses 4, 5, and 7 consisted of ifosfamide 9 g/m^2 and poside 500 mg/m^2 for previously untreated patients (34). The symbol "-" is used to indicate when selected information was not available. NSE: neuron ecific enolase.

ase #	Publication	Age (years)	Gender	Tumor location	Presenting symptoms	Imaging findings	Extent of resection	Adjuvant chemotherapy	Adjuvant radiation therapy	Clinical status	Length of follow-up	Histology	Immuno-histochemistry	Molecular findings
1	Tison et al., 1996 (ref 52)	24	M	left posterior fossa	headache, emesis, vertigo, impaired hearing	4 cm mass adherent to the tentorium and petrous portion of the temporal bone, with displacement of left cerebellar hemisphere; no extracranial malignancy on CT/MRI total body scans	subtotal	3 cycles consisting of PCNU, cisplatin, and VP-16 intracranial methotrexate every 40 days	yes	alive with no clinical signs of relapse at time of publication	~3 years	compact nests of small uniform round and oval cells with hyperchromatic nuclei and scarce cytoplasm, separated by a desmoplastic stroma, infrequent mitoses, with areas of necrosis	Desmin: positive EMA: positive Keratin: positive NSE: positive	PCR performed using *EWSR1* and *WT1* primers, *EWSR1-WT1* gene fusion detected by Southern blot
2	Bouchireb et al., 2008 (ref 9)	6	F	right temporal	headaches, complex partial seizure	well-dermarcated heterogeneously enhancing mass; PET-CT was negative for extracranial malignancy	gross total	MSKCC P6 protocol	focal conformal irradiation to the tumor bed with a 2 cm margin at 54 Gy	no evidence of disease	18 months	small round cell tumor with hyperchromatic nuclei and eosinophilic cytoplasm embeded in a fibromyxoid stroma, mitoses were infrequent	Desmin: positive EMA: negative AE1/ AE3: negative Synaptophysin: positive	*EWSR1-WT1* gene fusion detected by RT-PCR
3	Neder et al., 2009 (ref 40)	37	M	left cerebellopontine angle	left-sided hearing loss and tinnitus	heterogenouly enhancing mass, initial imaging suggested an acoustic neuroma; no	subtotal	after subsequent debulking of intradural spinal nodules, patient received	sterotactic irradiation to CPA tumor bed after subsequent debulking of	recurrent disease with spinal dissemination at 6 months, died at 2 years	2 years	sheets of small to medium sized cells with hyperchromatic nuclei and inconspicuous nucleoli, with a	Desmin: positive EMA: positive CAM 5.2: positive Synaptophysin: negative Neurofilament:	*EWSR1-WT1* gene fusion detected by RT-PCR

ase #	Publication	Age (years)	Gender	Tumor location	Presenting symptoms	Imaging findings	Extent of resection	Adjuvant chemotherapy	Adjuvant radiation therapy	Clinical status	Length of follow-up	Histology	Immuno-histochemistry	Molecular findings
						extracranial malignancy on CT/MRI total body scans		carboplatinum and temozolomide	intradural spinal nodules received brain and spinal irradiation, with radiosurgery to CPA			desmoplastic stroma, foci of necrosis mitotic index 5/10 HPFs	negative Ki-67 LI: 17.6%	
4	Neder et al., 2009 (ref 40)	39	M	posterior fossa	gait imbalance, bilateral lower limb weakness, with subsequent fall and hypotonic paraparesis	left cerebellar hemisphere, and CPA lesions with spinal leptomeningeal deposits at presentation, multiple patchy enhancing lesions	decompression of spinal cord	3 cycles of cisplatin, etoposide, and Holoxan	yes	alive with progressive disease	27 months	viable perivascular tumor cells seperated by necrosis, oval to irregular nuclei with coarse chromatin and scant cytoplasm, mitotic index 5/10 HPFs	Desmin: positive EMA: positive CAM 5.2: positive Synaptophysin: negative Neurofilament: negative Ki-67 LI: 11.5%	*EWSR1-WT1* gene fusion detected by RT-PCR
5	Thondam et al., 2015 (ref 50)	27	M	suprasellar	panhypopituitarism, with subsequent development of bitemporal hemianopia one year later after missing follow-up appointments	heterogenously enhancing suprasellar mass extending into third ventricle and the pituitary fossa; whole-body imaging was negative for extracranial malignancy	near total resection	palliative chemotherapy was considered, but the patient's clinical condition deteriorated	fractionated conformal radiotherapy was initiated at recurrence but discontinued due to clinical deterioration	tumor recurred at 4 months, followed by cervical and mediastinal lymph node metastases, patient died at 20 months	20 months	nests and cords of fairly uniform cells with hyperchromatic nuclei and indistinct cytoplasm distributed in a desmpolastic stroma, with calcifications and necrosis	Desmin: positive CAM 5.2: positive EMA: patchy CK7: focal CK20: focal NSE: focal Neurofilament: patchy	*EWSR1-WT1* gene fusion detected by RT-PCR
6	Al-Ibraheemi et al., 2017 (ref 2)	6	M	intracranial, infratemporal fossa	-	-	-	-	-	-	-	"Ewing sarcoma-like," small cell, desmoplasia present	Desmin: positive Cytokeratin: focal	*EWSR1-WT1* gene fusion detected by RT-PCR
7	Al-Ibraheemi et al., 2017 (ref 2)	37	M	cerebellopontine angle	-	-	-	yes	yes	vertebral metastasis, died with disease	32 months	"Ewing sarcoma-like," desmoplasia present	Desmin: positive Cytokeratin: positive	*EWSR1-WT1* gene fusion detected by RT-PCR